



OPEN

Skimmianine attenuates liver ischemia/reperfusion injury by regulating PI3K–AKT signaling pathway-mediated inflammation, apoptosis and oxidative stress

Cheng-long Huo, Bing Wang, Xuewen Zhang & Zhen-Gang Sun

Liver ischemia/reperfusion (I/R) injury is a common injury after liver transplantation and hepatectomy. Skimmianine (Ski) has antibacterial, antiviral pharmacological effects. However, it is not clear whether Ski has a protective effect against liver I/R injury. In the present study, we established a mouse liver I/R model and an AML12 cell hypoxia-reoxygenation (H/R) model, both pretreated with different concentrations of Ski. Serum transaminase levels, necrotic liver area, cell viability, inflammatory factors, oxidative stress and apoptosis-related levels were measured to assess the protective effect of Ski against liver I/R injury. Western blotting was used to detect apoptosis-related proteins and PI3K–AKT pathway-related proteins. Mice and cells were also treated with PI3K inhibitor LY294002 to assess changes in indicators of liver injury. The results showed that Ski significantly reduced transaminase levels, liver necrosis area, oxidative stress, and apoptosis levels in mice with I/R. Ski also inhibited cell injury and apoptosis after H/R. Moreover, Ski activated phosphorylation of PI3K–AKT pathway-related proteins after liver I/R and cell H/R. Importantly, the PI3K inhibitor LY294002 effectively reversed the alleviation of I/R injury caused by Ski. These results confirm that Ski exerts a protective effect against liver I/R injury through activation of the PI3K–AKT pathway.

Liver ischemia/reperfusion (I/R) injury is a pathophysiological process in which liver damage is further exacerbated after a period of ischemia in liver tissue followed by reperfusion of blood flow. Liver I/R injury commonly occurs after liver transplantation, hepatectomy and severe hemorrhagic shock^{1,2}. The mechanisms of liver I/R injury are complex, which include inflammatory damage, oxidation response, apoptosis, and endoplasmic reticulum stress as possible mechanisms of action³. During I/R injury, activation of Kupffer cells, macrophages, and mitochondrial damage promote reactive oxygen species (ROS) production and inflammatory responses, leading to liver tissue damage. A vicious cycle of ROS and oxidative stress, as well as mitochondrial dysfunction, contribute to the exacerbation of I/R injury^{4,5}. Apoptosis is a form of programmed cell death, and apoptosis also plays an important role in liver I/R injury⁶. Currently, there is a lack of very effective treatment modalities for liver I/R injury². Therefore, it is clinically important to explore a new and effective treatment to reduce liver I/R injury. The discovery of an effective drug that can reduce I/R injury in the liver could greatly contribute to the advancement of hepatobiliary surgery^{7,8}.

Phosphatidylinositol-3-kinase (PI3K) is an important molecule in the regulation of cell growth, metabolism and apoptosis. Protein kinase B (AKT), a serine-threonine kinase, is a kinase activated by phosphorylation. AKT is regulated by PI3K and exerts various effects on cellular processes including modulation of cellular inflammation, ROS, proliferation and apoptosis^{9,10}. It has been shown that activation of AKT attenuates the cellular inflammatory response and reduces apoptosis^{11,12}. Many studies have also demonstrated that activated AKT can attenuate I/R injury in the heart, kidney, brain, and liver^{10,13–15}.

Skimmianine is a natural furoquinoline alkaloid that can be obtained from plants of belonging to the Rutaceae family¹⁶. Some studies have shown that Ski has antibacterial, antiviral, pharmacological effects by inhibiting acetylcholinesterase and nitric oxide (NO) production^{17–19}. In addition, Ski has also been reported to have potent

Department of Hepatobiliary Surgery, Jingzhou Hospital Affiliated to Yangtze University, No. 26, Chuyuan Avenue, Jingzhou District, Jingzhou, Hubei, China. email: chrdwgd@163.com

anti-inflammatory effects. Its mechanism of action includes inhibition of TNF- α and IL-6 gene transcription, as well as inhibition of NO, prostaglandin E2 and superoxide anion production^{16,20}.

However, no studies have been reported on whether Ski can attenuate liver I/R injury. The further anti-inflammatory and antioxidant mechanisms of Ski also need to be further elucidated. In the present study, our group aimed to investigate the role of Ski on liver I/R injury and further mechanisms.

Materials and methods

Animals

Male C57BL/6J mice (6–8 weeks) were obtained from the Hubei Provincial Laboratory Animal Public Service Center (Wuhan, China). All animals were housed in a specific pathogen-free environment, had free access to food and water, and had a 12-h dark/light cycle. Mice were cared for according to NIH guidelines for laboratory animals. The study was carried out in compliance with the ARRIVE guidelines. Animal experiments were approved by the Ethics Committee of the Jingzhou Central Hospital.

Drug treatment and liver I/R injury model

Skimmianine (HY-N2081, MedChemExpress, Shanghai, China) was dissolved in 0.5% carboxymethyl cellulose sodium aqueous solution to different concentrations. Mice were randomly divided into sham-operated group, Ski group, I/R group and I/R + Ski group. The experiment was started after 14 days of continuous Ski gavage (once a day) prior to modeling, and the control group was given the same amount of dissolving solvent gavage. To further investigate the protective mechanism of Ski against liver I/R injury, PI3K inhibitor LY294002²¹ (20 mg/kg) was injected intraperitoneally 1 h prior to model in I/R + Ski + LY294002 group.

In this study, a 70% liver I/R injury model was established using mice²². Briefly, mice were anesthetized with an intraperitoneal injection of 1% sodium pentobarbital. After a median abdominal incision, the individual lobes of the liver were separated under the microscope and the vessels and bile ducts of the left and middle lobes of the liver were clamped using microvascular clips. After 1 h, the vascular clips were removed and reperfusion was initiated. The procedure in the sham-operated group was the same as that in the model group, but without vascular clamping of the liver. After 6 h of reperfusion, the mice were euthanized via cervical dislocation, and the absence of fluctuations in the thoracic cavity, respiration, and heart rate confirmed mortality. Then the tissues and blood specimens from the mice were obtained for further experiments.

Alanine aminotransferase (ALT) and aspartate aminotransferase (AST) assessments

After liver reperfusion, blood samples were collected from the orbit and left at room temperature for 30 min²³. Subsequently, serum was obtained by centrifuging the blood samples at 3500 g for 5 min. The obtained serum was used for the detection of serum levels of ALT and AST using the relevant kits (BC1555 and BC1565, Solarbio, Beijing, China).

Hematoxylin and eosin (HE) staining

Liver tissues were fixed in 10% formalin, embedded in paraffin, cut into 5 μ m thick paraffin sections. HE staining was performed according to the instructions for HE staining reagents (servicebio, Wuhan, China), observed under an inverted light microscope and photographed (Olympus, Japan)²⁴. The area of liver necrosis was analyzed by Image J.

Terminal deoxynucleotidyl transferase-mediated nick end labeling (TUNEL)

Five μ m Paraffin-embedded liver tissue sections were dewaxed, and each section was soaked by treating with 100 μ L proteinase K dropwise for 20 min at 37 °C in a wet box. After rinsing three times with PBS for 5 min each, TUNEL reaction solution was added dropwise and rinsed three times with PBS for 5 min each in a light-proof wet box at 37 °C²⁵. The nuclear were stained by DAPI. Sections were then sealed with an anti-fluorescence quencher and photographed under a fluorescent microscope (Olympus, Japan). The total number of cells and the number of positive cells (nuclei in red) were counted using Image J analysis software.

Cell culture and H/R model

AML12 cells were purchased from Procell Life Science & Technology Co., Ltd. (Wuhan, China) and cultured in Dulbecco's modified Eagle's medium/nutrient mixture F-12 medium (Procell, Wuhan, China) in a cell incubator with 5% CO₂ at 37 °C. AML12 cells from the H/R group were incubated in serum-free medium in a triple-gas incubator (5% CO₂, 94% N₂, 1% O₂) for 12 h to complete this step of hypoxia. Immediately after the completion of hypoxia, the serum-free medium was replaced with normal medium containing 10% fetal bovine serum (FBS) for reoxygenation, and the cells were placed in the normal incubator for 6 h to complete the reoxygenation²⁶.

Oxidative stress analysis

Mouse liver tissue or AML12 cells were homogenized with PBS or extract and centrifuged at 8000 g for 10 min. The supernatant was collected, and the protein concentration was quantified using the BCA Protein Concentration Assay Kit²⁷ (PC0020, Solarbio, Beijing, China). The malondialdehyde (MDA) level, Superoxide Dismutase (SOD), and Glutathione (GSH-Px) activities were detected according to the kit instructions (BC0025, BC0175 and BC1195, Solarbio, Beijing, China). Reactive oxygen species (ROS) generation in liver tissue was detected using dihydroethidium (DHE) staining (GDP1018, Servicebio, Wuhan, China). Briefly, fresh frozen liver tissue was cut into 10 μ m sections and incubated with DHE (10 μ M/L) at 37 °C for 30 min in the dark, and images were captured using a fluorescence microscope (Olympus, Japan)²⁸.

Cell counting kit-8 assay

AML12 cells were inoculated in 96-well plates at 5×10^3 cells per well²⁹, and the cells were treated with Ski or H/R. After 24 h of Ski treatment or after H/R treatment, 10 μ l of CCK-8 reagent (C0037, Beyotime, Shanghai, China) solution was added to each well of the plate and incubated for 1 h at 37 °C and 5% CO₂, the absorbance was measured by a micro-plate reader (Bio-Rad, USA) at 450 nm³⁰. The relative proliferation ratio was calculated by as follows: (experimental absorbance value/control absorbance value) \times 100%³¹. At least three independent tests were performed, each independent test included six wells.

Flow cytometry analysis

After reoxygenation, the culture medium was discarded. After washing with PBS once, the cells were digested using trypsin without EDTA to collect the cells, centrifuged at 200 g for 5 min, and 100 μ l suspension was added to resuspend the cells and stained with 5 μ l Anexin V-FITC and 5 μ l PI staining solution (CA1020, Solarbio, Beijing, China), which the cells were incubated in at room temperature for 15 min in the dark, and then detected by flow cytometry (BD Biosciences, USA)³².

Real-time polymerase chain reaction (PCR) analyses

Total RNA was isolated using Trizol reagent (Solarbio, Ltd, Beijing, China) according to the manufacturer's instructions, and 1 μ g of RNA per sample was reverse transcribed using the PrimerScript Reverse Transcription Kit (R323-01, Vazyme, Nanjing, China) according to the manufacturer's protocol. After reverse transcription, PCR reactions were performed using the SYBR qPCR Master (Mix reagent (Q711-02, Vazyme, Nanjing, China) kit. GAPDH was used as an internal reference, and the expression level of the target gene was calculated using the $2^{-\Delta\Delta C_t}$ ³³. The primers used in the experiments are listed in Table 1.

Western blotting

Total proteins were extracted using RIPA lysis buffer supplemented with a mixture of PMSE, peptidase and phosphatase inhibitors. Protein concentrations were measured using a BCA Protein Concentration Assay Kit (PC0020, Solarbio, Beijing, China). Proteins were separated using SDS-PAGE on 10% or 12% SDS gels (30 μ g per lane), transferred to PVDF membranes and incubated with primary antibodies at 4 °C overnight, followed by incubation with appropriate horseradish peroxidase (HRP)-coupled secondary antibodies for 1 h at room temperature. BeyoECL Plus (SA00001-1, Beyotime, Shanghai, China) was used for signal visualization. Images were collected using a Fushon Fx (Vilber Lourmat) imaging system (Marne-la-Vallée, France) (Original protein results are provided in Supplementary file).

Molecular docking

The two-dimensional structure of Skimmianine was drawn using Chemdraw (version 19.0; Cambridge soft corporation) and subsequently imported into Chemdraw 3D (version 15.0; Cambridge soft corporation) for energy minimization using the MM2 module to obtain the lowest energy advantage concept and saved as a mol 2 file. The PI3K protein structure (AF-Q3U6Q4) was downloaded from AlphaFold Protein Structure Database and subsequently visualized separately using PyMOL (The PyMOL Molecular Graphics System, version 2.0.6; Schrödinger, LLC), and then the ligand and receptor were saved separately as PDPQT using Mgtools 1.5.6³⁴ after processing by dehydration, hydrogen addition, charge calculation, and merging of non-polar hydrogen, etc. The docking of ligand and receptor was performed using Autodock vina 1.1.2³⁵ and visualized by PyMOL.

Statistical analysis

SPSS software (version 22.0; IBM Corp.) was used for statistical analyses. A one-way ANOVA followed by a post hoc Bonferroni correction was used for the statistical analysis more than two groups. A Student's t-test was used to compare the differences between two groups. $P < 0.05$ was considered to indicate a statistically significant difference.

Primer	Primer sequence
IL-1 β F	5'-TGCCACCTTTTGACAGTGATG-3'
IL-1 β R	5'-TGATGTGCTGCTGCGAGATT -3'
IL-6 F	5'-TGATGGATGCTACCAAACCTGGA-3'
IL-6 R	5'-TGTGACTCCAGCTTATCTCTTGG-3'
TNF- α F	5'-CCCTCACACTCACAACCAC-3'
TNF- α R	5'-ACAAGGTACAACCCATCGGC-3'
CXCL10 F	5'-TGCCGTCATTTCTGCCTCA-3'
CXCL10 R	5'-AGGCTCGCAGGGATGATTTC-3'
GAPDH F	5'-GGAGAGTGTTCCTCGTCCC-3'
GAPDH R	5'-ATGAAGGGTTCGTTGATGGC-3'

Table 1. Gene-specific quantitative-polymerase chain reaction primers.

Results

Skimmiannine attenuates liver I/R injury in mice

We treated different groups of mice with different concentrations of Ski and subsequently constructed a liver I/R injury model. The results showed that the levels of ALT and AST were significantly ($P < 0.01$) reduced in Ski treated mice, and the protective effect was most obvious in the 40 mg/kg group (Fig. 1A,B). Meanwhile, we performed HE staining on liver tissues of mice and counted the necrotic area. The results showed that the necrotic area of Ski-treated mice was significantly ($P < 0.01$) reduced compared to the I/R group (Fig. 1C,D). Therefore, in the subsequent experiments, we selected 40 mg/kg concentration of Ski for treatment. These results suggest that Ski could significantly reduce liver I/R injury.

Skimmiannine alleviates inflammation response in mouse liver I/R injury

We used PCR technique to detect the changes of IL1- β , IL-6, TNF α , and CXCL10 in mouse liver tissues. The results showed that Ski treatment could significantly ($P < 0.01$) attenuate IL1- β , IL-6, TNF α , CXCL10 levels after I/R compared with the I/R group alone (Fig. 2A–D). Meanwhile, we performed myeloperoxidase (MPO) staining of liver tissues from mice using immunohistochemistry, and the results also showed that Ski treatment significantly ($P < 0.01$) attenuated MPO expression after I/R (Fig. 2E,F). These results suggest that Ski reduced the inflammatory response in liver I/R injury.

Skimmiannine alleviates oxidative stress after liver I/R in mice

To detect the level of oxidative stress in mice after liver I/R, we measured the levels of SOD, GSH-Px and MDA in the liver tissues. The results showed that Ski treatment significantly ($P < 0.01$) reduced the elevated MDA levels induced by I/R, while increased SOD and GSH-Px activity caused by I/R compared with the I/R group (Fig. 3A–C). Meanwhile, we performed DHE staining to detect ROS content in mouse liver tissues, and the results confirmed that Ski could significantly ($P < 0.01$) reduce the ROS content after I/R injury (Fig. 3D,E). These results suggested that Ski can reduce oxidative stress in liver I/R injury.

Skimmiannine alleviates apoptosis in mouse liver after I/R

To further investigate whether Ski can affect the level of apoptosis after liver I/R injury. We performed TUNEL staining on mouse liver tissue, and the results showed that Ski treatment significantly ($P < 0.01$) reduced the percentage of TUNEL positive cells compared with the I/R group alone (Fig. 4A,B). Meanwhile, we detected apoptosis-related proteins in mouse livers. The results showed that Ski treatment could significantly ($P < 0.01$) reduce the protein expression levels of Bax and Cleaved-caspase3 after liver I/R injury. Correspondingly, Ski significantly ($P < 0.01$) elevated the protein expression level of Bcl-2 in liver after I/R injury (Fig. 4C,D). For mice without I/R treatment, Ski did not exert a significant effect. These results suggest that Ski alleviated the elevated apoptosis caused by I/R injury.

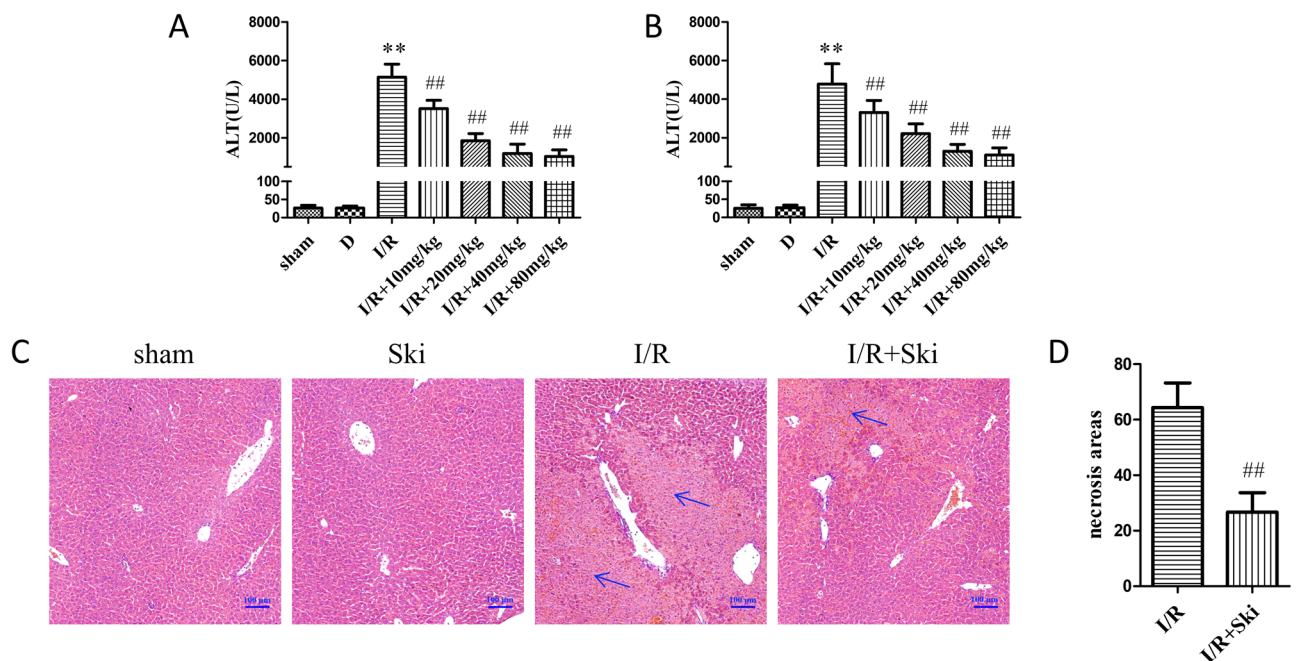


Figure 1. Skimmiannine attenuates liver I/R injury in mice. (A and B) Serum ALT and AST contents of mice in different treatment groups. (C) Representative H&E staining and (D) necrotic area statistical analysis of liver tissue. ** $P < 0.01$ versus sham group; ## $P < 0.01$ versus I/R group.

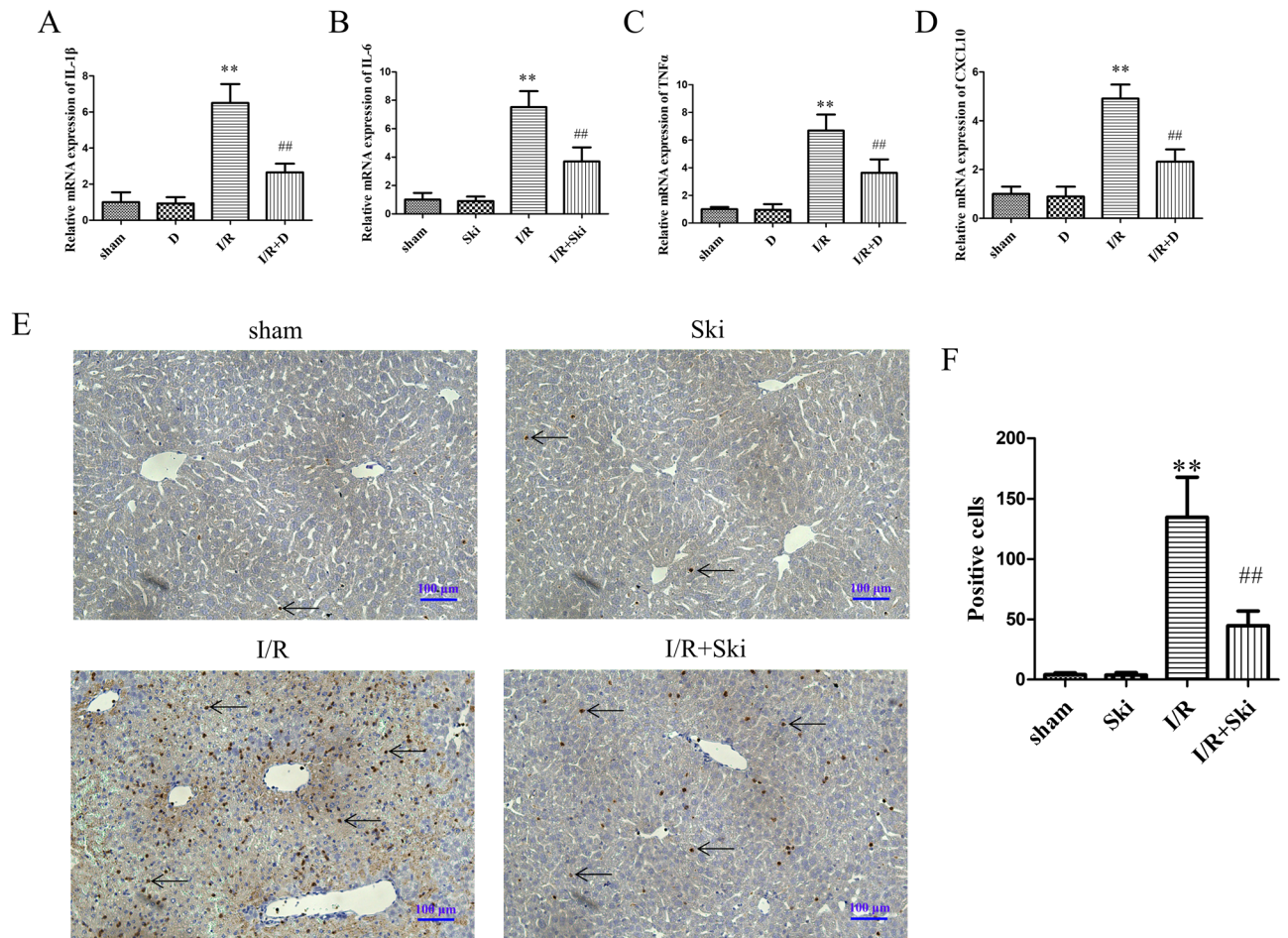


Figure 2. Skimmianine alleviates inflammation in mouse liver I/R injury. (A–D) The mRNA expression of inflammatory cytokines IL-1 β , IL-6, TNF- α , and CXCL10 of mice in different treatment groups. (E) Representative MPO immunohistochemical staining of liver tissues and (F) statistical analysis from different groups. ** $P < 0.01$ versus sham group; ## $P < 0.01$ versus I/R group.

Skimmianine alleviates H/R-induced cell injury

We first treated the AML12 cell line with different concentrations of Ski and determined the cell viability by CCK-8 assay after 24 h of treatment. The results showed that Ski concentrations of 40 μ M and below had no significant ($P > 0.05$) damaging effect on the AML12 cell line (Fig. 5A). Therefore, in the next H/R cell treatment, we used Ski concentrations below 40 μ M for cell treatment. By performing CCK-8 assay on the cells after H/R, we found that Ski at 40 μ M provided the most significantly ($P < 0.01$) protection to the cells after H/R (Fig. 5B). Therefore, subsequent cell assays were performed using 40 μ M Ski for treatment. We measured the percentage of apoptosis in cells after H/R using flow cytometry and demonstrated that Ski significantly ($P < 0.01$) reduced the increase in apoptosis due to H/R (Fig. 5C,D). Correspondingly, we measured apoptosis-related proteins. The results showed that Ski significantly ($P < 0.01$) reduced the protein expression of Bax and Cleaved-caspase3 compared to the H/R group, while Ski significantly ($P < 0.01$) enhanced the protein expression of Bcl-2 (Fig. 5E,F). These results suggest that Ski could attenuate the cell damage caused by H/R and reduce apoptosis after H/R.

Skimmianine activates PI3K–AKT pathway after liver I/R

The PI3K/AKT signaling pathway plays a crucial role in regulating inflammation, oxidative stress, and apoptosis following liver ischemia–reperfusion injury. Previous studies have indicated a potential link between Skimmianine and the PI3K pathway, suggesting that Skimmianine may be associated with the modulation of this pathway³⁶. We docked PI3K with Ski using molecular docking. The results revealed that Ski was able to bind effectively to the active pocket of PI3K with a binding energy of -6.3 kcal/mol, indicating that Ski is able to bind PI3K more spontaneously (Fig. 6A)³⁷. Furthermore, we examined PI3K–AKT pathway proteins in mouse liver tissues after I/R injury. Our results showed that Ski could significantly ($P < 0.01$) activate the expression of phosphorylated PI3K (p-PI3K) as well as phosphorylated AKT (p-AKT) in mice after I/R injury, but the expression of total PI3K as well as AKT proteins did not change significantly ($P > 0.05$) (Fig. 6B,C). Meanwhile, we also obtained the same results in the H/R model of AML12 cells. Ski significantly ($P < 0.01$) activate the expression of p-PI3K as well as p-AKT in AML12 cells after H/R, but the expression of total PI3K as well as AKT protein was

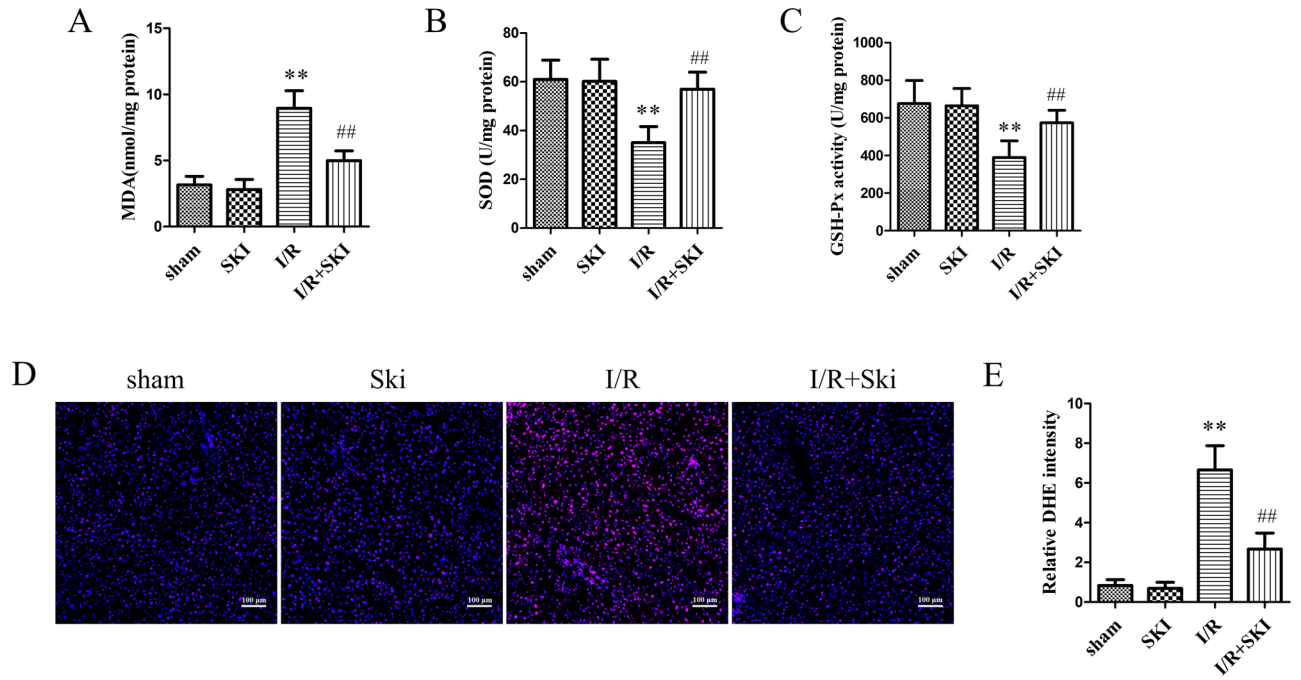


Figure 3. Skimmianine alleviates oxidative stress after liver I/R in mice. (A) MDA content, (B) SOD activity and (C) GSH-Px activity in liver tissues of mice in different treatment groups (D) Representative DHE staining and (E) fluorescence intensity statistical analysis of liver tissues in different treatment mice. ** $P < 0.01$ versus sham group; * $P < 0.05$ and ## $P < 0.01$ versus I/R group.

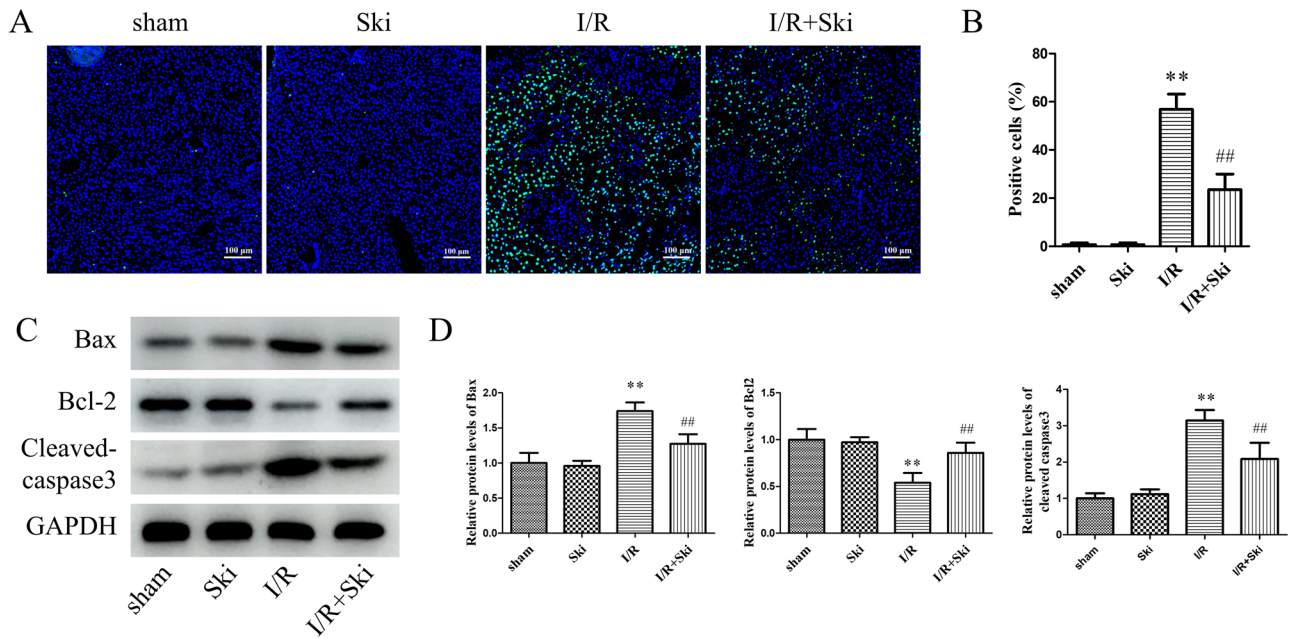


Figure 4. Skimmianine alleviates apoptosis in mouse liver after I/R. (A, B) TUNEL staining and statistical analysis of liver tissue in different treatment mice. (C) The protein expression of Bax, Bcl-2 and Cleaved-caspase 3 and (D) protein quantitative analysis of liver tissue in different treatment mice. ** $P < 0.01$ versus sham group; ## $P < 0.01$ versus I/R group.

not significantly ($P > 0.05$) changed (Fig. 6D,E). These evidences suggest that Ski could activate the inhibition of PI3K–AKT pathway in mouse liver I/R injury.

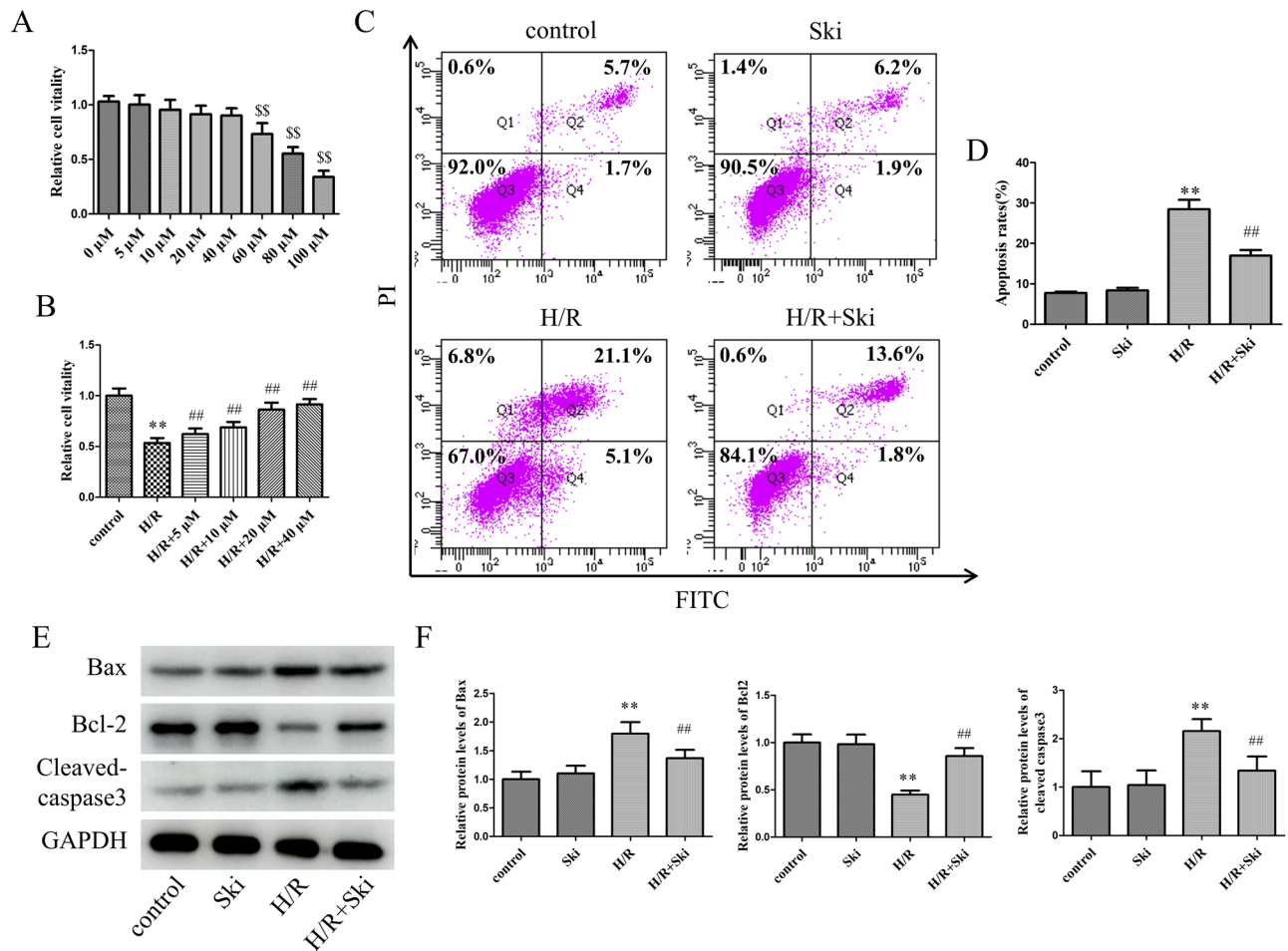


Figure 5. Skimmianine alleviates H/R-induced cell injury. (A) Effect of different concentrations of Ski on the activity of AML12 cells under normoxia. (B) Effects of different concentrations of Ski on the activity of AML12 cells under H/R. (C and D) Apoptosis rate detection and statistical analysis by flow cytometry. (E) The protein expression of Bax, Bcl-2 and Cleaved-caspase 3 and (F) protein quantitative analysis in different treatment cells. $^{SS}P < 0.01$ versus 0 μM group; $^{**}P < 0.01$ versus control group; $^{##}P < 0.01$ versus H/R group.

Skimmianine inhibits liver I/R injury via PI3K–AKT pathway

To further verify whether Ski exerts a protective effect against liver I/R via the PI3K–AKT pathway. We used LY294002, an inhibitor of PI3K, to treat mice with intraperitoneal injection. The results showed that LY294002 could well reverse the decrease of ALT and AST levels caused by Ski ($P < 0.01$) (Fig. 7A,B). Also LY294002 could reverse the reduction of liver I/R necrotic area caused by Ski ($P < 0.01$) (Fig. 7C,D). We also confirmed that LY294002 reversed the reduction of inflammation-related indicators IL1- β , IL-6, TNF α and CXCL10 caused by Ski ($P < 0.01$) (Fig. 7E–H). In terms of oxidative stress, LY294002 reversed the reduction of oxidative stress-related indicators MDA, and the elevation of SOD and GSH caused by Ski ($P < 0.01$) (Fig. 7I–K). More importantly, LY294002 reversed the Ski-induced decrease in liver I/R TUNEL positive cells ($P < 0.01$) (Fig. 7L,M). These results could indicate that Ski exerts a protective effect on liver I/R injury via PI3K–AKT pathway.

Discussion

Cellular inflammatory response, apoptosis, and oxidative stress are important mechanisms of liver I/R injury³⁸. Therefore, it is particularly important to find drugs to reduce inflammation, apoptosis, and oxidative stress after liver I/R.

Direct indicators of liver damage are ALT and AST levels in the serum, and the area of liver damage under pathological sections can also be a good indicator of the extent of liver damage^{39,40}. In this study, we first demonstrated that Ski was able to attenuate the levels of ALT and AST and necrotic area in mouse liver after I/R injury. These results are direct evidence that Ski attenuates liver I/R injury in mice. Inflammatory injury plays an important role in liver I/R injury, and inflammation-related markers such as IL1- β , IL-6, TNF α , and CXCL10 are often elevated in mouse I/R⁴¹. MPO has been shown to be a local mediator of inflammation caused by tissue damage and in various inflammatory diseases⁴². Our study confirms that Ski reduces the mRNA expression of IL1- β , IL-6, TNF α , CXCL10 and infiltration of MPO inflammatory cells. These results suggest that Ski exerts an anti-inflammatory effect in liver I/R injury.

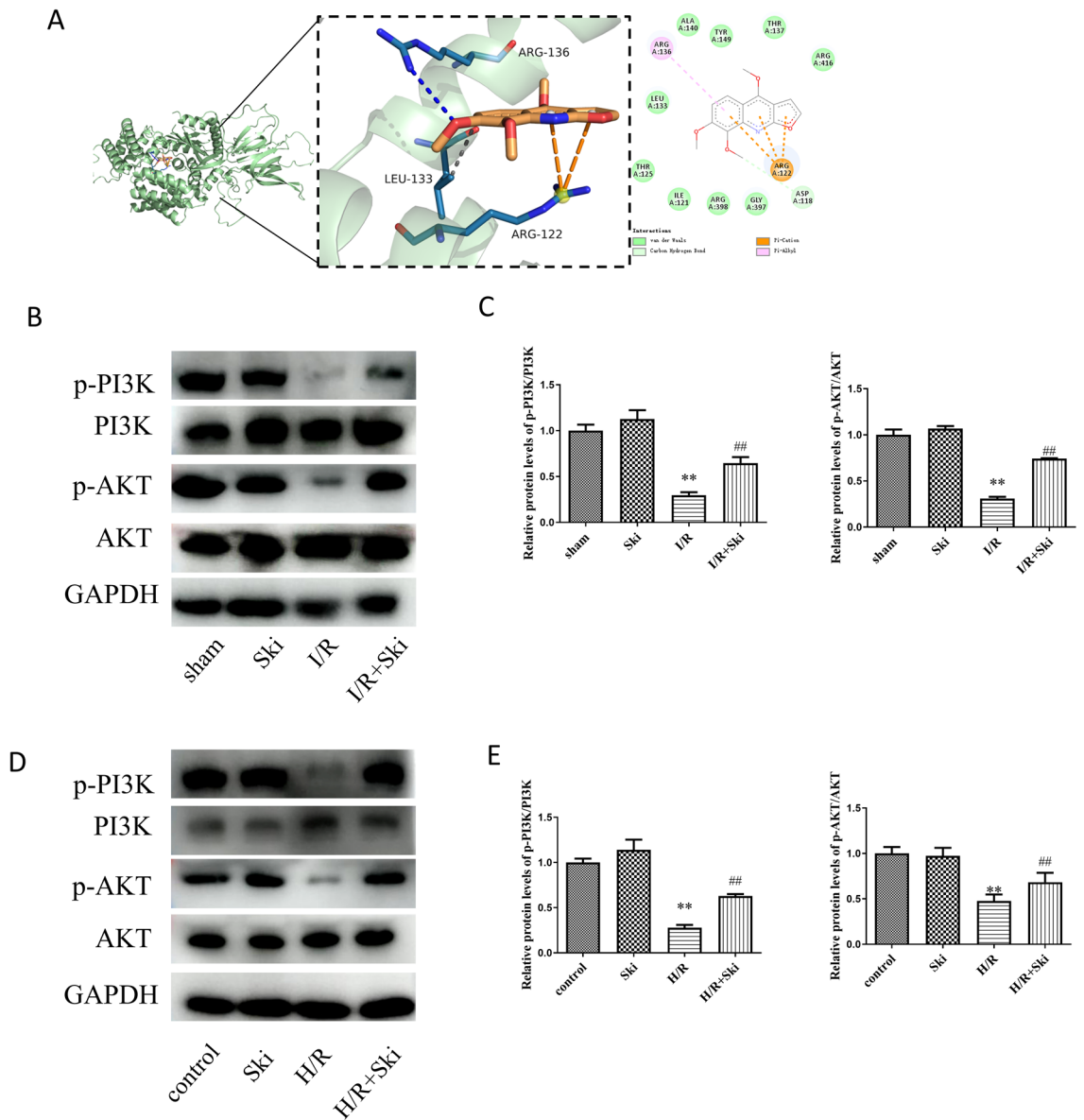


Figure 6. Skimmiarine activates PI3K–AKT pathway after liver I/R. **(A)** The docking results of Ski and PI3K molecules. **(B)** The protein expression of p-PI3K, PI3K, p-AKT, AKT and **(C)** protein quantitative analysis in different treatment mice. **(D)** The protein expression of p-PI3K, PI3K, p-AKT, AKT and **(E)** protein quantitative analysis in different treatment cells. * $P < 0.01$ versus sham group; ** $P < 0.01$ versus I/R group; ## $P < 0.01$ versus control group; && $P < 0.01$ versus H/R group.

Oxidative stress also plays an important function in liver I/R injury. Related indicators such as SOD, GSH-Px, MDA, and DHE staining can detect ROS content^{2,38}. We demonstrated in this study that Ski attenuates the production of oxidative stress-related products after liver I/R. This indicates that Ski is able to attenuate liver I/R injury by inhibiting oxidative stress.

Many studies have confirmed the important role of apoptosis in liver injury as well as in liver I/R injury. Targeting the mitigation of apoptosis levels through pharmacological interventions is a promising strategy to cope with liver I/R injury^{1,43–45}. Correspondingly, we confirmed the increased apoptosis after I/R injury and cellular H/R model. Also, our results suggest that Ski inhibits the onset of apoptosis in I/R injury. These evidences confirm that Ski can attenuate liver I/R injury by inhibiting apoptosis.

To further investigate the mechanism by which Ski attenuates liver I/R injury. Many studies have confirmed that the PI3K–AKT pathway can play a pivotal role in liver I/R injury^{10,22}. Specifically, PI3K–AKT pathway is inhibited in liver I/R injury and activation of PI3K–AKT pathway can reduce liver I/R injury^{46,47}. Meanwhile, we learned from research that Ski may interact with PI3K³⁶. To further confirm our conjecture, we used molecular docking for validation. Molecular docking is a very effective method for finding drug binding targets. The literature shows that a docking score of less than -7.0 indicates a strong binding ability of the target to the compound, scores between -5.0 and -7.0 indicates a good binding ability of the small molecule to the target, and scores

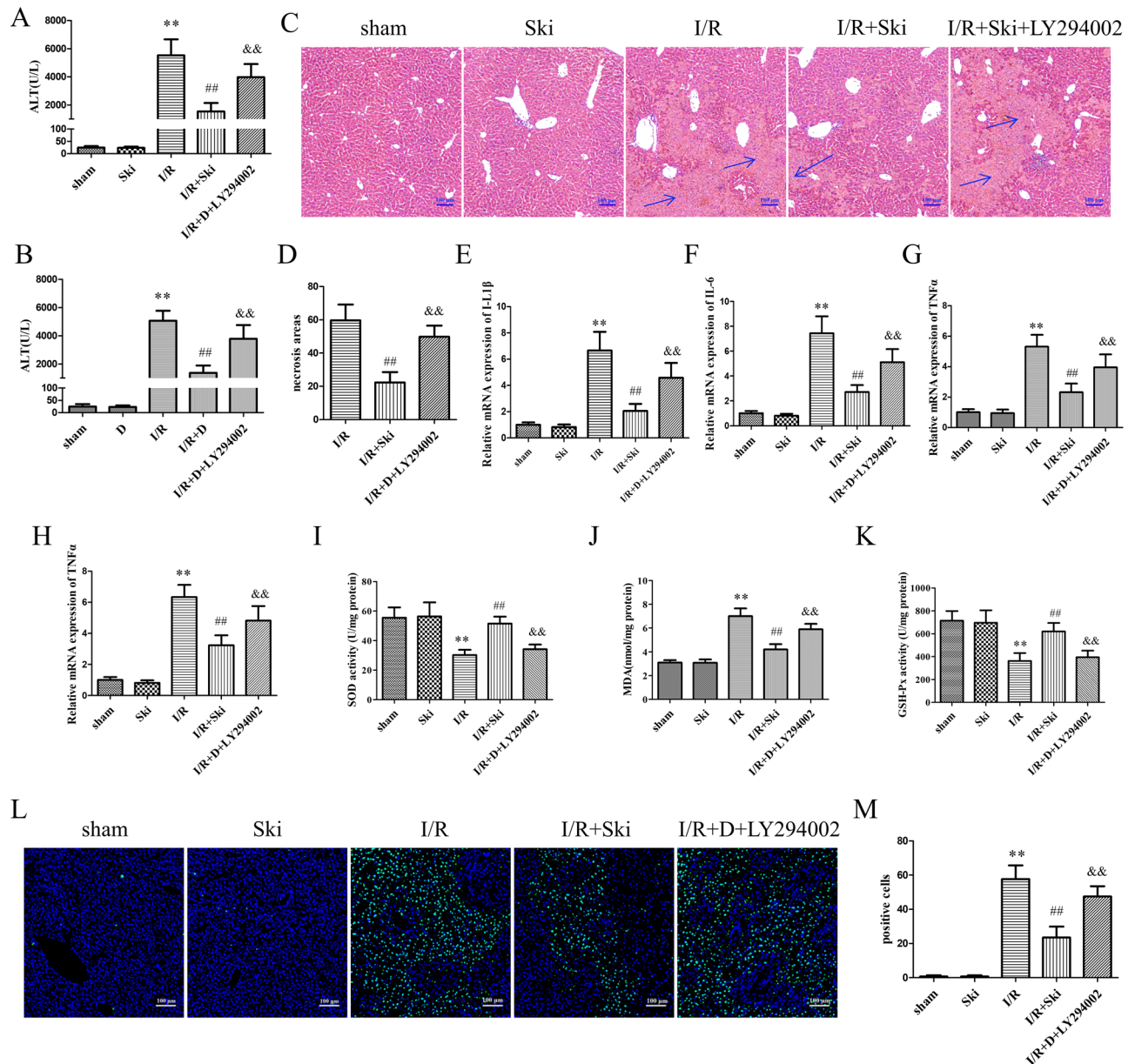


Figure 7. Skimmianine inhibits liver I/R injury via PI3k-AKT pathway. (A and B) Serum ALS and AST contents of mice in different treatment groups, (C) representative H&E staining and (D) necrotic area statistical analysis of liver tissue, (E–H) The mRNA expression of inflammatory cytokines IL-1 β , IL-6, TNF- α , and MCP-1 of mice in different treatment groups; (I–K) MDA content, SOD activity and GSH activity in liver tissues of mice in different treatment groups. (L, M) TUNEL staining and statistical analysis of liver tissue in different treatment mice. ** $P < 0.01$ versus sham group; ## $P < 0.01$ versus I/R group; && $P < 0.01$ versus I/R + Ski group.

between -5.0 and -4.25 indicates a certain binding ability of the compound to the target^{48,49}. We docked PI3K with Ski using molecular docking. Ski was able to bind effectively to the active pocket of PI3K with a binding energy of -6.3 kcal/mol, indicating that Ski is able to bind PI3K more spontaneously. Meanwhile, the WB results further confirmed that Ski could activate the PI3K-AKT pathway.

To further confirm the mechanism of Ski action with hepatic I/R injury. We employed LY294002, a known inhibitor of PI3K phosphorylation, to treat mice. LY294002 could inhibit PI3K phosphorylation and thus act to inactivate PI3K. The results showed that LY294002 could reverse the attenuation of liver I/R injury caused by Ski. These results confirm that Ski exerts a protective effect against liver I/R injury through activation of the PI3K-AKT pathway.

In conclusion, our study confirm that Ski can alleviate inflammation, apoptosis and oxidative stress after hepatic I/R injury, and that Ski exerts its protective effect on hepatic I/R injury through the PI3K-AKT signaling pathway (Fig. 8). We have made an important contribution by being the first to demonstrate the protective effect of Skimmianine on hepatic I/R injury. This finding opens up a new potential avenue for drug treatment of hepatic I/R injury. Our research provides valuable insights into the therapeutic potential of Ski and highlights its

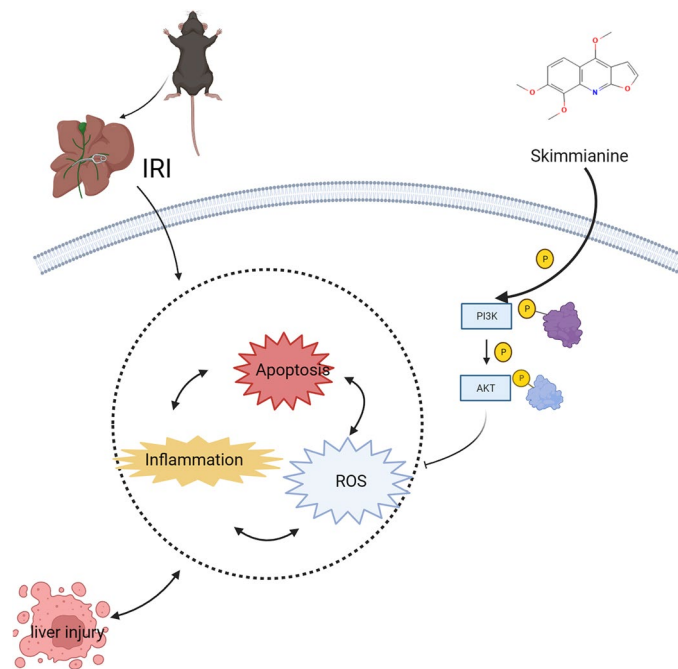


Figure 8. Schematic diagram of the role of Skimmianine in regulating the PI3k–AKT pathway against I/R-induced liver injury.

significance as a candidate for further exploration and development in the field of hepatic I/R injury treatment. However, the direct effect of Ski on hepatic I/R injury, and whether Ski can reduce hepatic I/R injury through other pathways needs to be further investigated.

Data availability

The datasets generated during and/or analyzed during the current study are available from the corresponding author on reasonable request.

Received: 21 February 2023; Accepted: 18 October 2023

Published online: 25 October 2023

References

- Ye, L. *et al.* Effect of hepatic macrophage polarization and apoptosis on liver ischemia and reperfusion injury during liver transplantation. *Front. Immunol.* **11**, 1193 (2020).
- Cannistrà, M. *et al.* Hepatic ischemia reperfusion injury: A systematic review of literature and the role of current drugs and biomarkers. *Int. J. Surg. (Lond. Engl.)* **33**(Suppl 1), S57–70 (2016).
- Konishi, T. & Lentsch, A. B. Hepatic ischemia/reperfusion: Mechanisms of tissue injury, repair, and regeneration. *Gene Expr.* **17**, 277–287 (2017).
- Peralta, C., Jiménez-Castro, M. B. & Gracia-Sancho, J. Hepatic ischemia and reperfusion injury: effects on the liver sinusoidal milieu. *J. Hepatol.* **59**, 1094–1106 (2013).
- Tang, S. P. *et al.* Reactive oxygen species induce fatty liver and ischemia-reperfusion injury by promoting inflammation and cell death. *Front. Immunol.* **13**, 870239 (2022).
- Zhang, S. *et al.* Role of mitochondrial pathways in cell apoptosis during Hepatic ischemia/reperfusion injury. *Int. J. Mol. Sci.* **23**, 2357 (2022).
- Shi, S. & Xue, F. Current antioxidant treatments in organ transplantation. *Oxidative Med. Cell. Longev.* **2016**, 8678510 (2016).
- Bavarsad, K. *et al.* Protective effects of curcumin against ischemia-reperfusion injury in the liver. *Pharmacol. Res.* **141**, 53–62 (2019).
- Suo, L. *et al.* Carvacrol alleviates ischemia reperfusion injury by regulating the PI3K–Akt pathway in rats. *PLoS ONE* **9**, e104043 (2014).
- Meng, F. *et al.* PI3K/AKT activation attenuates acute kidney injury following liver transplantation by inducing FoxO_{3a} nuclear export and deacetylation. *Life Sci.* **272**, 119119 (2021).
- Wu, Y., Fan, L., Wang, Y., Ding, J. & Wang, R. Isorhamnetin alleviates high glucose-aggravated inflammatory response and apoptosis in oxygen-glucose deprivation and reoxygenation-induced HT22 hippocampal neurons through Akt/SIRT1/Nrf₂/HO-1 signaling pathway. *Inflammation* **44**, 1993–2005 (2021).
- Fisher, L. Retraction: Salvianolic acid B inhibits inflammatory response and cell apoptosis via the PI3K/Akt signaling pathway in IL-1 β -induced osteoarthritis chondrocytes. *RSC Adv.* **11**, 4441 (2021).
- Bi, X. *et al.* Endoplasmic reticulum chaperone GRP78 protects heart from ischemia/reperfusion injury through Akt activation. *Circ. Res.* **122**, 1545–1554 (2018).
- Liu, B., Deng, Q., Zhang, L. & Zhu, W. Nobiletin alleviates ischemia/reperfusion injury in the kidney by activating PI3K/AKT pathway. *Mol. Med. Rep.* **22**, 4655–4662 (2020).

15. Li, Y. *et al.* Protection against acute cerebral ischemia/reperfusion injury by Leonuri Herba total alkali via modulation of BDNF-TrkB-PI3K/Akt signaling pathway in rats. *Biomed. Pharmacother.* **133**, 111021 (2021).
16. Ratheesh, M., Sindhu, G. & Helen, A. Anti-inflammatory effect of quinoline alkaloid skimmianine isolated from *Ruta graveolens* L.. *Inflamm. Res. Off. J. Eur. Histamine Res. Soc.* **62**, 367–376 (2013).
17. Kiplimo, J. J., Islam, M. S. & Koorbanally, N. A. A novel flavonoid and furoquinoline alkaloids from *Vepris glomerata* and their antioxidant activity. *Nat. Prod. Commun.* **6**, 1847–1850 (2011).
18. Hanawa, F., Fokialakis, N. & Skaltsounis, A. L. Photo-activated DNA binding and antimicrobial activities of furoquinoline and pyranoquinolone alkaloids from rutaceae. *Planta Med.* **70**, 531–535 (2004).
19. Cheng, J. T., Chang, T. K. & Chen, I. S. Skimmianine and related furoquinolines function as antagonists of 5-hydroxytryptamine receptors in animals. *J. Auton. Pharmacol.* **14**, 365–374 (1994).
20. Huang, A. *et al.* Metabolic profile of skimmianine in rats determined by ultra-performance liquid chromatography coupled with quadrupole time-of-flight tandem mass spectrometry. *Molecules (Basel, Switz.)* **22**, 489 (2017).
21. Qian, B., Yao, Z., Yang, Y., Li, N. & Wang, Q. Downregulation of SDCBP inhibits cell proliferation and induces apoptosis by regulating PI3K/AKT/mTOR pathway in gastric carcinoma. *Biotechnol. Appl. Biochem.* **69**, 240–247 (2022).
22. Li, S. *et al.* TSLP protects against liver I/R injury via activation of the PI3K/Akt pathway. *JCI Insight* **4**, e129013 (2019).
23. Li, Y., Zhu, J. & Tang, J. Computational systems pharmacology and molecular docking reveal an anti-apoptosis and anti-inflammatory mechanism of compound Angelica Ligusticum Wallichii Granules in the treatment of endometriosis. *Drug Des. Dev. Ther.* **17**, 743–759 (2023).
24. Yu, Q. *et al.* Mitogen activated protein kinase phosphatase 5 alleviates liver ischemia-reperfusion injury by inhibiting TAK1/JNK/p38 pathway. *Sci. Rep.* **13**, 11110 (2023).
25. Wang, Y. *et al.* miR-130a alleviates neuronal apoptosis and changes in expression of Bcl-2/Bax and caspase-3 in cerebral infarction rats through PTEN/PI3K/Akt signaling pathway. *Exp. Ther. Med.* **19**, 2119–2126 (2020).
26. Li, J. *et al.* KLF6 alleviates hepatic ischemia-reperfusion injury by inhibiting autophagy. *Cell Death Dis.* **14**, 393 (2023).
27. Xu, F. *et al.* Attenuation of doxorubicin-induced cardiotoxicity by esculetin through modulation of Bmi-1 expression. *Exp. Ther. Med.* **14**, 2216–2220 (2017).
28. Hu, C. *et al.* Fibronectin type III domain-containing 5 improves aging-related cardiac dysfunction in mice. *Aging Cell* **21**, e13556 (2022).
29. Li, X. *et al.* Study on the potential mechanism of tonifying kidney and removing dampness formula in the treatment of postmenopausal dyslipidemia based on network pharmacology, molecular docking and experimental evidence. *Front. Endocrinol.* **13**, 918469 (2022).
30. Ying, L. *et al.* Paracrine FGFs target skeletal muscle to exert potent anti-hyperglycemic effects. *Nat. Commun.* **12**, 7256 (2021).
31. Chai, J. *et al.* Overexpression of KAI1/CD82 suppresses in vitro cell growth, migration, invasion and xenograft growth in oral cancer. *Mol. Med. Rep.* **15**, 1527–1532 (2017).
32. Park, T. S., Zimmerlin, L. & Zambidis, E. T. Efficient and simultaneous generation of hematopoietic and vascular progenitors from human induced pluripotent stem cells. *Cytom. Part A J. Int. Soc. Anal. Cytol.* **83**, 114–126 (2013).
33. Liu, X. *et al.* Honokiol induces paraptosis-like cell death of acute promyelocytic leukemia via mTOR & MAPK signaling pathways activation. *Apoptosis Int. J. Program. Cell Death* **26**, 195–208 (2021).
34. Morris, G. M. *et al.* AutoDock4 and AutoDockTools4: Automated docking with selective receptor flexibility. *J. Comput. Chem* **30**, 2785–2791 (2009).
35. Trott, O. & Olson, A. J. AutoDock Vina: Improving the speed and accuracy of docking with a new scoring function, efficient optimization, and multithreading. *J. Comput. Chem.* **31**, 455–461 (2010).
36. Wu, N. *et al.* Network pharmacology and molecular docking study of the Chinese Miao medicine Sidaxue in the treatment of rheumatoid arthritis. *Drug Des. Dev. Ther.* **16**, 435–466 (2022).
37. Hsin, K. Y., Ghosh, S. & Kitano, H. Combining machine learning systems and multiple docking simulation packages to improve docking prediction reliability for network pharmacology. *PLoS ONE* **8**, e83922 (2013).
38. Bi, J. *et al.* Irisin alleviates liver ischemia-reperfusion injury by inhibiting excessive mitochondrial fission, promoting mitochondrial biogenesis and decreasing oxidative stress. *Redox Biol.* **20**, 296–306 (2019).
39. Aljobaily, N. *et al.* Creatine alleviates doxorubicin-induced liver damage by inhibiting liver fibrosis, inflammation, oxidative stress, and cellular senescence. *Nutrients* **13**, 41 (2020).
40. Shang, L. *et al.* SS-31 Protects liver from ischemia-reperfusion injury via modulating macrophage polarization. *Oxidative Med. Cell. Longev.* **2021**, 6662156 (2021).
41. Yang, Q. *et al.* Senkyunolide I attenuates hepatic ischemia/reperfusion injury in mice via anti-oxidative, anti-inflammatory and anti-apoptotic pathways. *Int. Immunopharmacol.* **97**, 107717 (2021).
42. Aratani, Y. Myeloperoxidase: Its role for host defense, inflammation, and neutrophil function. *Arch. Biochem. Biophys.* **640**, 47–52 (2018).
43. Liu, D. Q. *et al.* Berberine protects against ischemia-reperfusion injury: A review of evidence from animal models and clinical studies. *Pharmacol. Res.* **148**, 104385 (2019).
44. Lin, J. *et al.* The effect of Ginsenoside Rg1 in hepatic ischemia reperfusion (I/R) injury ameliorates ischemia-reperfusion-induced liver injury by inhibiting apoptosis. *Biomed. Pharmacother.* **129**, 110398 (2020).
45. Shen, Y., Shen, X., Cheng, Y. & Liu, Y. Myricitrin pretreatment ameliorates mouse liver ischemia reperfusion injury. *Int. Immunopharmacol.* **89**, 107005 (2020).
46. Wu, Y. *et al.* Dexmedetomidine alleviates hepatic ischaemia-reperfusion injury via the PI3K/AKT/Nrf2-NLRP3 pathway. *J. Cell. Mol. Med.* **25**, 9983–9994 (2021).
47. Li, Y., Tong, L., Zhang, J., Zhang, Y. & Zhang, F. Galangin alleviates liver ischemia-reperfusion injury in a rat model by mediating the PI3K/AKT pathway. *Cell. Physiol. Biochem. Int. J. Exp. Cell. Physiol. Biochem. Pharmacol.* **51**, 1354–1363 (2018).
48. Ferreira, L. G., Dos Santos, R. N., Oliva, G. & Andricopulo, A. D. Molecular docking and structure-based drug design strategies. *Molecules (Basel, Switz.)* **20**, 13384–13421 (2015).
49. Pinzi, L. & Rastelli, G. Molecular docking: Shifting paradigms in drug discovery. *Int. J. Mol. Sci.* **20**, 4331 (2019).

Author contributions

C.H. and Z.-G.S. conceived and designed research; C.H., B.W. and X.Z. performed the experiments and data analysis; C.H. drafted manuscript; C.H. and B.W. edited and revised manuscript; Z.-G.S. and X.Z. approved the final version of manuscript.

Competing interests

The authors declare no competing interests.

Additional information

Supplementary Information The online version contains supplementary material available at <https://doi.org/10.1038/s41598-023-45354-2>.

Correspondence and requests for materials should be addressed to Z.-G.S.

Reprints and permissions information is available at www.nature.com/reprints.

Publisher's note Springer Nature remains neutral with regard to jurisdictional claims in published maps and institutional affiliations.



Open Access This article is licensed under a Creative Commons Attribution 4.0 International License, which permits use, sharing, adaptation, distribution and reproduction in any medium or format, as long as you give appropriate credit to the original author(s) and the source, provide a link to the Creative Commons licence, and indicate if changes were made. The images or other third party material in this article are included in the article's Creative Commons licence, unless indicated otherwise in a credit line to the material. If material is not included in the article's Creative Commons licence and your intended use is not permitted by statutory regulation or exceeds the permitted use, you will need to obtain permission directly from the copyright holder. To view a copy of this licence, visit <http://creativecommons.org/licenses/by/4.0/>.

© The Author(s) 2023